RESEARCH ARTICLE

Title: A High Voltage, Multi Output, Quasi Resonant Design of Flyback DC-DC Converter

Yash Wadhavana*, Dr. A.A. Apte*

*Department of Electrical Engineering AISSMS College of Engineering Pune Maharashtra India

ABSTRACT:

Introduction/Objective: High-voltage auxiliary power supplies require compact, efficient, and reliable multi-output DC–DC converters capable of operating over wide input ranges. Conventional hard-switched flyback converters suffer from high switching losses, electromagnetic interference (EMI), and device stress. This study aims to design and validate a quasi-resonant (QR) multi-output flyback converter using SiC technology to improve efficiency and robustness.

Methods: A 66 W isolated QR flyback converter operating over a 250–820 V DC input range is developed using a 1200 V SiC MOSFET and a QR controller enabling valley switching. A custom interleaved multi-winding transformer is designed to minimize leakage inductance and improve cross-regulation across seven outputs. The system incorporates RCD snubber circuits, optocoupler-based feedback control, and selective post-regulation. Performance is evaluated through simulation and experimental validation, focusing on voltage stress, regulation accuracy, and dynamic response.

Results: The converter demonstrates stable operation across the full input range with reliable startup characteristics. Output voltages remain within specified limits under varying load conditions. Peak MOSFET voltage stress is limited to approximately 1.1–1.2 kV, ensuring safe operation. Leakage energy is effectively controlled, reducing switching losses and EMI while maintaining consistent cross-regulation across outputs.

Discussion: The integration of QR control with SiC devices significantly enhances efficiency and reduces device stress compared to conventional approaches. The multi-winding transformer design effectively mitigates cross-regulation challenges.

Conclusion: The proposed converter achieves high efficiency, compact design, and robust performance, making it suitable for industrial and high-voltage auxiliary applications, with scope for further improvement using advanced topologies.

Keywords: Flyback converter; quasi-resonant switching; SiC MOSFET; multi-output isolated DC–DC; high dv/dt; wide input.

1. INTRODUCTION

High-voltage auxiliary power supplies in traction systems, industrial drives, grid-tied converters, and power-electronics test infrastructure increasingly demand compact, robust, and efficient DC–DC solutions with wide input compliance and multiple isolated rails. Flyback topology remains attractive in the ≤100 W range for its simplicity, inherent isolation, and ease of generating multiple outputs. However, ultra-wide input ranges (≥3:1), multi-output cross-regulation, and EMI/thermal constraints necessitate careful device selection, magnetic design, and control strategy. This work describes a 66 W QR flyback that operates from 250–820 V DC, enabled by a 1200 V SiC MOSFET and a QR controller (ICE5X1XSD). The overarching design goals are: (i) safe operation at high line with valley switching and controlled device stresses; (ii) tight regulation of seven isolated outputs; (iii) predictable loop dynamics across the operating envelope; and (iv) manageable thermal and EMI performance within a compact form factor. Measured results and simulations substantiate the design choices and quantify margins.

2. LITERATURE REVIEW

2.1 Flyback converters are extensively used in isolated DC–DC power conversion for low-to-medium power levels due to their simple structure, low component count, and inherent ability to provide galvanic isolation and voltage scaling. Their suitability for generating multiple isolated outputs from a single transformer further enhances their widespread adoption in auxiliary, control, and embedded power supplies. 2.2 Despite their advantages, hard-switched flyback converters suffer from high switching losses, significant voltage stress across the primary switch, and increased electromagnetic interference (EMI). These drawbacks become more pronounced at higher switching frequencies, limiting achievable power density and efficiency. 2.3 To overcome these limitations, quasi-resonant (QR) flyback converters have been introduced. By turning on the primary switch at the drain–source voltage valley, QR converters achieve near zero-voltage switching, which reduces turn-on losses and improves overall efficiency. 2.4 In QR flyback operation, switching frequency varies with load and input voltage conditions. This adaptive frequency control improves light-load efficiency but introduces challenges related to frequency spread, transformer design constraints, and acoustic noise at light loads. 2.5 Soft-switching mechanisms in QR flyback converters significantly reduce switching losses and alleviate stress on the power semiconductor devices. This enables higher switching frequencies, leading to reduced magnetic component size and improved power density. 2.6 Wide-bandgap (WBG) semiconductors, particularly silicon carbide (SiC) MOSFETs, have gained prominence in power electronics due to their superior electrical and thermal characteristics compared to silicon MOSFETs, including higher breakdown voltage, lower switching losses, and high-temperature capability. 2.7 Application of SiC MOSFETs in flyback converters has demonstrated substantial reductions in switching losses and improved high-frequency operation. Their fast-switching capability makes them particularly well suited for QR flyback topologies. 2.8 Several recent studies report that combining QR control with SiC MOSFETs enables efficiencies exceeding those of silicon-based flyback converters, particularly under wide input voltage ranges and high switching frequency operation. 2.9 The ability of SiC MOSFETs to operate efficiently at high switching frequencies allows significant reduction in transformer size and magnetic losses. This directly contributes to higher power density and compact converter design. 2.10 Multi-winding flyback converters provide multiple isolated output voltages using a single magnetic structure. This approach reduces cost, volume, and complexity compared to multiple single-output converters. 2.11 One of the major challenges in multi-winding flyback converters is cross-regulation, where load variation on one output affects the voltage regulation of other outputs. This issue is exacerbated by unequal leakage inductances and coupling coefficients among windings. 2.12 Increased leakage inductance in multi-winding flyback transformers leads to higher voltage spikes, switching stress, and efficiency degradation. Proper winding arrangement and optimized transformer design are essential to mitigate these effects. 2.13 Various passive and active snubber circuits, such as RCD clamps, active clamps, and self-driven snubbers, have been proposed to limit voltage stress caused by leakage inductance. However, passive snubbers introduce additional losses, while active solutions increase circuit complexity. 2.14 Recent research indicates that quasi-resonant operation can partially mitigate voltage stress and switching losses in multi-winding flyback converters. However, resonant behaviour must be carefully managed to ensure consistent operation across all outputs. 2.15 Control of multi-output QR flyback converters remains challenging due to variable switching frequency, load-dependent dynamics, and cross-regulation effects. Primary-side regulation techniques and digital control strategies have been explored but are not yet fully optimized. 2.16 SiC-based multi-winding QR flyback converters are increasingly considered for applications such as electric vehicle auxiliary supplies, industrial gate-driver power supplies, renewable-energy control circuits, and telecom systems, all of which demand high efficiency, compactness, and wide input voltage operation. 2.17 While previous works individually address SiC devices, quasi-resonant control, or multi-winding flyback structures, comprehensive studies integrating all three aspects remain limited. Experimental validation of efficiency, voltage stress reduction, and cross-regulation performance is sparse. 2.18 Motivated by the identified research gaps, this work focuses on the design, implementation, and experimental evaluation of a SiC-based multi-winding quasi-resonant flyback DC–DC converter, emphasizing transformer design, efficiency optimization, and voltage stress reduction under wide operating conditions.

*Address correspondence to this author at Department of Electrical Engineering AISSMS College of Engineering Pune Maharashtra India

Tel: +91 8758683668 Email: jobandyash@gmail.com

3. SYSTEM DETAILS

The Block Diagram of Flyback Converter Fig 1 is explained specifying the function of each block. The proposed flyback DC–DC converter uses an isolated single-switch topology with a primary-side control IC (IC600) driving a power MOSFET (Q200) as shown in Schematic Fig 2. The DC input is stabilized by bulk electrolytic capacitors (C600, C601) and high-frequency ceramic bypass capacitors, while startup resistors (R219, R223) provide initial bias to IC600 until the auxiliary winding sustains operation. In steady state, IC600 operates Q200 in peak current-mode PWM, with precision current-sense resistors (R618, R620) enabling cycle-by-cycle current limiting, soft-start, and fault protection. Voltage stress from transformer leakage inductance is controlled using an RCD snubber (R603, C602, D605) and additional damping networks around TR600 to reduce ringing and EMI. Energy is stored in the transformer magnetizing inductance during the MOSFET on-time and transferred to the secondary during off-time through rectifier diodes (D606A/D607), with the output filtered by bulk and ceramic capacitors for low ripple and fast transient response. Output regulation is achieved via a secondary-side reference (DZ200) and optocoupler feedback, providing accurate

closed-loop control while maintaining galvanic isolation across wide line and load conditions.

The system is a 66 W isolated multi-output QR flyback converter operating from a 250–820 V DC input, providing +24 V, +25 V×3, +17 V, +7 V, and −19 V outputs, with regulation referenced to the +25 V rail and post-regulation on +7 V and +17 V. It uses an Infineon IMWH170R450M1 1200 V SiC MOSFET driven by the ICE5X1XSD QR controller, implementing valley switching, frequency fold-back, burst/skip operation, and comprehensive protections (UVLO, OCP/OLP, brown-in/out, short-circuit). Operation is QR with variable frequency at low/mid line, shifts toward DCM at high line to reduce peak current, and enters burst mode at light load for efficiency and acoustic control. A custom interleaved P-S-P-S transformer is designed to limit reflected voltage VR=n(Vo+Vd) so that VDS,max≈Vin,max+VR remains well within the 1200 V limit at 820 V input, while Lm is selected to balance peak current, frequency spread, and power transfer, with interleaving minimizing leakage, clamp loss, and EMI. Leakage energy is handled by an RCD or RC+TVS clamp, rectification is optimized per rail (Schottky/ultrafast/SiC), TL431/opto Type-II compensation ensures stable control with ~50–60° phase margin, and careful layout, creepage/clearance, and CM/DM filtering enable EMI compliance and thermal margin.

4. RESULTS

Input-Voltage Range and Regulation : At 24 °C, as shown in Fig 3 , the converter reliably starts at ~62 V DC (Level 1), maintains regulation down to ~60 V under maximum load (Level 2), and ceases operation below ~22–24 V (Level 3), while withstanding DC input voltages up to ~855–863 V without failure (Level 4). As shown in Fig 4 & 5, the outputs remain within specification, with P17F at 16.82–17.06 V and P24M1 at 20.23–25.52 V depending on load.

Secondary Diode Surge and Capacitor RMS Stress: As shown in Fig 6 , Table 1 and Table 2 and Table 3 , For P24M1, peak current is ~8.52 A at max load (11.5 Ω) and ~3.94 A at min load (150 Ω), with peak diode voltage ~137–141 V; capacitor RMS current and reverse voltage remain well within limits. For P17F, peak current is ~2.31–2.45 A with ~92.4 V peak diode voltage, while average consumption, surge, and thermal margins meet specifications. Simulation results were also matching the design requirements for Vds , Vo, I, IL1 and IL2 as shown in figure 7.

Switching Device and Clamp Stress: At ~760 V DC bus, MOSFET V_DS peak ≈ 1.10 kV (≈600 V headroom vs. 1.7 kV rating); RCD clamp ≈ 1.03 kV vs. 2 kV limit (≈968 V margin). Primary current remained below the design limit (1.83 A measured vs. 2.05 A spec). At ~820 V (OBF), V_DS peak ≈ 1.196 kV (≈504 V margin), clamp ≈ 1.112 kV (≈888 V margin). Minimum-line (~230 V) showed benign stresses (V_DS peak ≈ 530 V, RCD ≈ 464 V). A representative nominal switching frequency of ~49.8 kHz was observed.

FIGURES AND TABLES

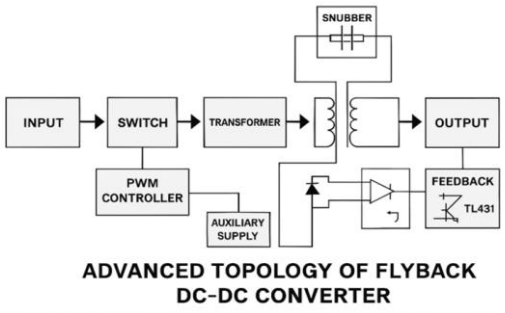

Fig. (1). Block Diagram: Flyback DC DC Converter

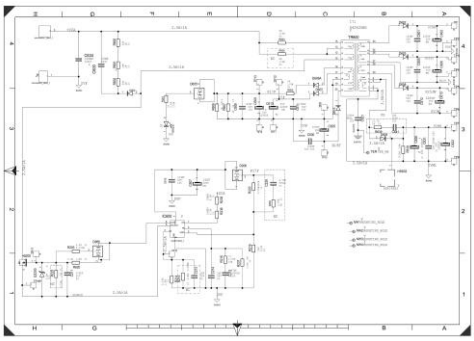

Fig. (2). Schematic Diagram of the circuit

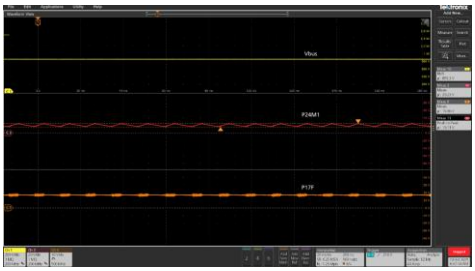

Fig. (3). Output Regulation of P24M1 and P17F at Maximum Load

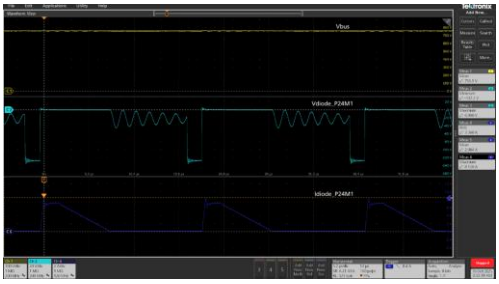

Fig. (4). P24M1 Diode Voltage and Current at Maximum Load

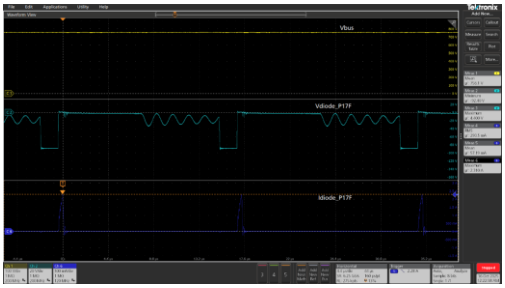

Fig. (5). P17F Diode Voltage and Current at Maximum Load

Fig. (6). Snubber Voltage, Switching Voltage and Primary Current at Nominal input Voltage of 760V

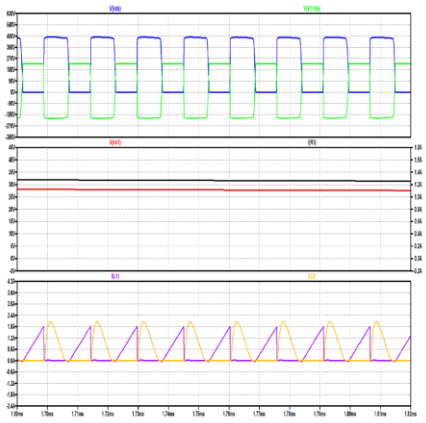

Fig. (7). Simulation results for Vds, output Voltage V0 , Output current I0 and Primary Current (IL1) and Secondary Current (IL2).

Table 1. Secondary Diode and Capacitor Current for P24M1

Load Condition	Load	Idrms (A)	Idc (A)	Icrms (A)	Ipeak (A)	Vd peak (V)
Maximum Load	11.5 Ω	3.36	2.084	2.64	8.52	137.2
Minimum Load	150 Ω	0.636	0.181	0.609	3.94	141.2
User + Options	47 Ω	1.354	0.517	1.251	5.90	139.6

Table 2. Secondary Diode and Capacitor Current for P17F

Load Condition	Load	Idrms (A)	Idc (A)	Icrms (A)	Ipeak (A)	Vd peak (V)
Maximum Load	11.5 Ω	0.290	0.057	0.284	2.310	92.40
Minimum Load	150 Ω	0.236	0.058	0.229	1.930	92.40
User + Options	47 Ω	0.287	0.061	0.280	2.45	92.40

Table 3. DCM behavior at the operating point of 760v DC

Merit	Value
V(BR)DS (SiC MOSFET)	1700 V
Measured VDS peak	1100 V
Margin to V(BR)DSS	600 V
Primary I peak (spec vs. measured)	2.05 A vs. 1.83 A
RCD Clamp V peak	1032 V
Margin to RCD Diode VR	968 V

5. CONCLUSION

A compact 66 W multi-output QR flyback converter is demonstrated for a wide 250–820 V input using a 1200 V SiC MOSFET and ICE5X1XSD controller. Valley switching, interleaved magnetics, and selective post-regulation ensure stable seven-output regulation, controlled stresses, and solid thermal/EMI performance. Tests confirm reliable operation, wide input tolerance, and strong component margins. Future work includes active-clamp flyback and synchronous rectification.

LIST OF ABBREVIATIONS

Abbreviation	Meaning
VR	Voltage Ratio
CM	Common Mode
DM	Differential Mode
EMI	Electromagnetic Interference
Id	Diode Current, A
Idc	DC Current, A
Ic	Collector Current, A
I	Load Current, A
Vd	Diode Voltage, V
Vds	Drain to Source Voltage, V
VBR	Breakdown Voltage , V

REFERENCES

[1] Z. Li, Z. Zhao, K. Dong, D. Gao, F. Feng, and G. Teng, "Design of quasi-resonant forward–flyback DC/DC converter based on SiC MOSFET," in *Lecture Notes in Electrical Engineering*, Springer, 2024.
[2] J. S. Lai, B. Y. Chen, and Y. S. Lai, "A high-efficiency quasi-resonant flyback DC–DC converter with reduced switch voltage stress using an active snubber," *IEEE Transactions on Power Electronics*, vol. 38, no. 3, pp. 3121–3132, Mar. 2023.
[3] F. Jiang, Y. Nie, X. Ma, and H. Liu, "Design and implementation of a SiC MOSFET-based flyback converter for high-voltage auxiliary power supplies," in *Proc. IEEE Energy Conversion Congress and Exposition (ECCE)*, 2021, pp. 1–7.
[4] S. H. Özen, U. E. Doğru, R. Ö. Yaşar, and E. Akboy, "Multiple-output quasi-resonant flyback converter for television power supply applications," in *Proc. International Conference on Electrical and Electronics Engineering (ELECO)*, 2023, pp. 215–220.
[5] B. Yang, Y. Wang, and D. Jiang, "Transformer design and optimization for multi-winding quasi-resonant flyback converters," *IEEE Transactions on Industry Applications*, vol. 58, no. 6, pp. 6894–6904, Nov.–Dec. 2022.
[6] Y. Zhang, Z. Lu, and Z. Chen, "Analysis and efficiency improvement of quasi-resonant flyback converters under wide input voltage operation," *IEEE Transactions on Power Electronics*, vol. 39, no. 2, pp. 1645–1656, Feb. 2024.
[7] W. Zhou and X. Yuan, "Experimental evaluation of SiC MOSFETs in a soft-switching flyback converter," *IEEE Transactions on Industry Applications*, vol. 57, no. 5, pp. 5130–5140, Sept.–Oct. 2021.
[8] H. W. Kim and J. H. Park, "Design and evaluation of a multi-output flyback DC–DC converter using wide-bandgap devices," *Journal of Power Electronics*, vol. 22, no. 4, pp. 1221–1230, 2022.
[9] H. Jia, W. Hu, Y. Song, P. Mao, and Z. Shen, "Design and analysis of a quasi-resonant dual-switch four-winding flyback converter," *Electrical Engineering*, vol. 108, Art. no. 232, Springer, 2026.
[10] L. Corradini, P. Mattavelli, and S. Saggini, "High-frequency isolated DC–DC converter using SiC MOSFETs for electric vehicle auxiliary supplies," *IEEE Transactions on Transportation Electrification*, vol. 7, no. 3, pp. 1624–1635, Sept. 2021.
[11] R. Zelnik and M. Praženica, "Voltage stress suppression techniques for multi-winding flyback converters operating in quasi-resonant mode," in *Proc. International Conference on Electronics*, 2021, pp. 98–103.
[12] D. W. Kim and M. H. Lee, "Design considerations of quasi-resonant flyback converters using wide bandgap semiconductor devices," *IEEE Access*, vol. 8, pp. 178945–178956, 2020.
[13] B. Zhu, Y. Yang, K. Wang, J. Liu, and D. M. Vilathgamuwa, "High transformer utilization ratio flyback converter for photovoltaic applications," *IEEE Transactions on Industry Applications*, vol. 60, no. 2, pp. 2840–2851, Mar.–Apr. 2024.
[14] Y. Ying, J. Zeng, R. Hu, and S. Liu, "A soft-switching high-voltage-gain DC–DC converter with quasi-resonant operation," *Journal of Power Electronics*, vol. 22, no. 8, pp. 1120–1130, 2022.
[15] H. Kong, S. Mihara, K. Sato, and J. Suno, "Single-switch quasi-resonant DC–DC converter for space power applications," in *Proc. IEEE Aerospace Conference*, 2021, pp. 1–8.